pISSN 2384-1095
eISSN 2384-1109

iMRI 2019;23:202-209

https://doi.org/10.13104/imri.2019.23.3.202

iMRI
Investigative Magnetic Resonance Imaging

Ultrashort Echo Time MRI (UTE-MRI) Quantifications of Cortical Bone Varied Significantly at Body Temperature Compared with Room Temperature

Saeed Jerban[1], Nikolaus Szeverenyi[1], Yajun Ma[1], Tan Guo[1], Behnam Namiranian[1], Sarah To[2], Hyungseok Jang[1], Eric Y. Chang[1,2], Jiang Du[1]

[1]Department of Radiology, University of California, San Diego, United States
[2]Radiology Service, VA San Diego Healthcare System, San Diego, United States

Original Article

Received: January 25, 2019
Revised: March 12, 2019
Accepted: March 26, 2019

Correspondence to:
Jiang Du, M.D.
Department of Radiology, University of California, 9500 Gilman Dr., San Diego, CA 92093, USA.
Tel. +1-858-246-2248
Fax. +1-888-960-5922
E-mail: jiangdu@ucsd.edu

Saeed Jerban, M.D.
Department of Radiology, University of California, 9500 Gilman Dr., San Diego, CA 92093, USA.
Tel. +1-858-246-3158
Fax. +1-888-960-5922
E-mail: sjerban@ucsd.edu

Purpose: To investigate the temperature-based differences of cortical bone ultrashort echo time MRI (UTE-MRI) biomarkers between body and room temperatures. Investigations of *ex vivo* UTE-MRI techniques were performed mostly at room temperature however, it is noted that the MRI properties of cortical bone may differ *in vivo* due to the higher temperature which exists as a condition in the live body.
Materials and Methods: Cortical bone specimens from fourteen donors (63 ± 21 years old, 6 females and 8 males) were scanned on a 3T clinical scanner at body and room temperatures to perform T1, T2*, inversion recovery UTE (IR-UTE) T2* measurements, and two-pool magnetization transfer (MT) modeling.
Results: Single-component T2*, IR-T2*, short and long component T2*s from bi-component analysis, and T1 showed significantly higher values while the noted macromolecular fraction (MMF) from MT modeling showed significantly lower values at body temperature, as compared with room temperature. However, it is noted that the short component fraction (Frac1) showed higher values at body temperature.
Conclusion: This study highlights the need for careful consideration of the temperature effects on MRI measurements, before extending a conclusion from *ex vivo* studies on cortical bone specimens to clinical *in vivo* studies. It is noted that the increased relaxation times at higher temperature was most likely due to an increased molecular motion. The T1 increase for the studied human bone specimens was noted as being significantly higher than the previously reported values for bovine cortical bone. The prevailing discipline notes that the increased relaxation times of the bound water likely resulted in a lower signal loss during data acquisition, which led to the incidence of a higher Frac1 at body temperature.

Keywords: Cortical bone; Magnetic resonance imaging; Ultrashort echo time; Body temperature

INTRODUCTION

Generally speaking, magnetic resonance imaging (MRI) has been increasingly used for cortical bone imaging and assessment, due to the relatively safe nature of MRI as compared to methods which use ionizing radiation, such as with computed tomography

(CT) (1-3). The dense and well-organized structure of the cortical bone results in short transverse magnetization decay (T2) of approximately 0.42-0.50 ms (4, 5); therefore, the clinical MRI sequences with TEs of several milliseconds gives rise to a negligible signal as seen from the cortical bone.

Ultrashort echo time (UTE) MRI can image and quantitatively assess cortical bone (2, 3, 6-17). At this juncture, the UTE-MRI can acquire signal several microseconds after radiofrequency (RF) excitation, before major T2 decay of cortical bone has occurred (4, 5). Dual echo UTE acquisition with echo subtraction, long T2 saturation UTE imaging, UTE with off-resonance saturation as well as single and dual adiabatic inversion recovery UTE techniques are examples of the now possible UTE-MRI techniques for high contrast imaging of cortical bone (4-6, 17). Several quantitative UTE-MRI techniques have been developed to assess cortical bone microstructure and mechanics. Broadly speaking, these techniques include T1 (18, 19), single-, bi-, and tricomponent analysis of apparent transverse relaxation time (T2*) (7, 14, 20), magnetization transfer ratio (MTR) (21), and magnetization transfer (MT) modeling from the macromolecules to water, which enabled measurement of the macromolecular protons fraction (MMF) (22, 23). These UTE biomarkers have demonstrated correlations with the noted key mechanical properties of the cortical bone. Specifically, short-T2* fraction from bi-component T2* analysis has been found to be positively associated with bone strength and toughness (14). In this case, the MMF from two-pool UTE-MT modeling as well as MTR have demonstrated significant correlations with human bone porosity, as measured with ultra-high resolution CT (μCT) (9, 21). Additionally, the incidence of significant MMF variation has been observed in cortical bone after bone stress injury, which is likely due to an induction of microcracks (24).

In this context, the UTE-MRI correlations with bone microstructure and mechanics have been examined routinely *ex vivo* at room temperature, yet the target bone for future clinical *in vivo* studies resides at body temperature. As reported in the literature, it is noted that the MRI properties in cortical bone and other tissues are functions of the temperature (25-29). In general, the results show that the tissue relaxation times increase with a noted temperature increase. Consequently, applying results of UTE-MRI techniques based on *ex vivo* results cannot be directly applied to *in vivo* studies without considering the effect of temperature. Of course, the differences between *in vivo* cortical bone and *ex vivo* tissues are not limited to just the measurement of the temperature in this case.

The main objective of this study was to investigate variation of UTE-MRI quantifications of cortical bone between scans at room temperature and scans at body temperature. In this study, the UTE techniques utilized in this study included single- and bi-component T2* fittings, inversion recovery UTE (IR-UTE) T2*, T1, and two-pool MT modeling that have been the recent focus of our research group.

MATERIALS AND METHODS

Regulated Temperature Air Blower

An MR compatible device was designed and manufactured in-house to force a directed air flow with a regulated temperature on the specimens during MRI scans. It consisted of a modified hair dryer and included a digital proportional-integral-derivative (PID) temperature controller (Red by Kiss Handle-less and MyPIN Universal Digital Controller) housed in a shielded aluminum box having a waveguide snout and aluminum screen for air exit and intake. There was also a flexible water pipe insulation tubing with a 2" internal diameter which was used to conduct the thermostated air from a safe location on the floor near the mouth of the magnet to the sample. The thermocouple tasked with providing feedback to the temperature controller was located approximately one foot from the exit snout inside the insulated tubing, resulting in the continued and stable regulation of the set temperature at this location, but with the thermal losses in the hose and sample housing, it was found necessary to set the temperature value 1.5 degree C higher to achieve the appropriately desired body temperature in the sample.

Sample Preparation

In this case, the cortical bone specimens were harvested from fourteen human tibial and femoral midshafts (63 ± 21 years old, 6 females and 8 males), which were provided by a nonprofit whole-body donation company (United Tissue Network, Phoenix, AZ, USA). To begin with, the tibial and femoral midshafts were cut into 30 mm segments using a commercial band saw. After the removal of the bone marrow, a rectangular strip was excised from each specimen using a low-speed diamond saw (Isomet 1000, Buehler, IL, USA), having the approximate dimensions of 4 × 2 × 30 mm.

UTE-MR Imaging

In what follows, all bone specimens were immersed in phosphate-buffered saline (PBS) for twelve hours at room temperature before the MRI scans. Then specimens were placed in a 30-mL syringe filled with perfluoropolyether (Fomblin, Ausimont, Thorofare, NJ, USA) to minimize dehydration and susceptibility artifacts. The UTE-MRI scans were performed on a 3T clinical scanner (MR750, GE Healthcare, Waukesha, WI, USA) using a homemade 1-inch diameter transmit/receive birdcage coil. Next, the scans were performed first at body temperature (i.e., 37.5˚C) and again at room temperature (19˚C). It is emphasized that the UTE scans involved the four following quantitative protocols: A) five sets of dual-echo 3D-UTE-Cones sequences (repetition time [TR] = 24.3, echo times [TEs] = 0.032, 0.2, 0.4, 0.8, 2.2, 4.4, 6.6, 8.8, 11 and 15 ms) for T2* single- and bi-component analyses, B) five set of 3D-inversion recovery (IR)-UTE-Cones sequence (inversion time [TI] = 45, TR = 100, TEs = 0.032, 0.2, 0.4, 0.6 and 1 ms, flip angle [FA] = 20˚) for IR-T2* measurements, C) an actual FA variable TR (AFI-VTR) sequence (AFI: TE = 0.032, TRs = 20 and 100 ms, VTR: TE = 0.032, TRs = 20, 50, 150 ms, FA = 45˚) for T1 measurements (19), which is a prerequisite for MT modeling, and D) a set of 3D-UTE-Cones-MT sequences (MT saturation pulse power = 400°, 600°, and 800°, frequency offset = 2, 5, 10, 20, and 50 kHz, FA = 10˚) for two-pool MT modeling (22, 23, 30). Other imaging parameters included: field of view (FOV) = 40 mm × 40 mm, matrix = 160 × 160, slice thickness = 3 mm, receiver bandwidth = ± 62.5 kHz. Features of the 3D-UTE-Cones sequence have been described in previous studies (31-33). The two-pool UTE-MT modeling was previously described in detail by Ma et al. (22, 23, 30).

Quantitative UTE-MRI Analyses

The quantitative MR analyses included single- and bi-component T2*, single-component IR-T2* and T1 as well as the two-pool MT modeling. The signal in single-component fitting of T2* and IR-T2* was modeled using the equation, $S(TE) \propto Exp(-TE/[\![T2]\!]\_\hat{}*)+constant$, where S(TE) is the normalized UTE-MRI or IR-UTE signal. For bi-component T2* fitting, a short T2* component (T2*1) and a long T2* component (T2*2) were assumed. The signal in bi-component fitting was modeled using the equation, $S(TE) \propto Frac1 \times Exp(-TE/[\![T2]\!]\_1\hat{}*)+ Frac2 \times Exp(-TE/[\![T2]\!]\_2\hat{}*)+constant$, where Frac1 and Frac2 are proton fractions of short and long T2* components, respectively.

T1 measurement was performed using the single-component fitting model, $S(TR) \propto (1-exp(-TR/T1)) +$ constant, where S (TR) is the normalized UTE-MRI signal (4, 5, 34).

The UTE-MT analysis was accomplished by using a two-pool model to estimate MMF and macromolecular T2 (T2MM) based on a modified rectangular pulse approximation approach (22, 23, 30). In the two-pool model, the first pool is macromolecular proton pool which has a very broad spectrum or extremely short T2 (~10 us), while the second pool is seen as a water proton pool which

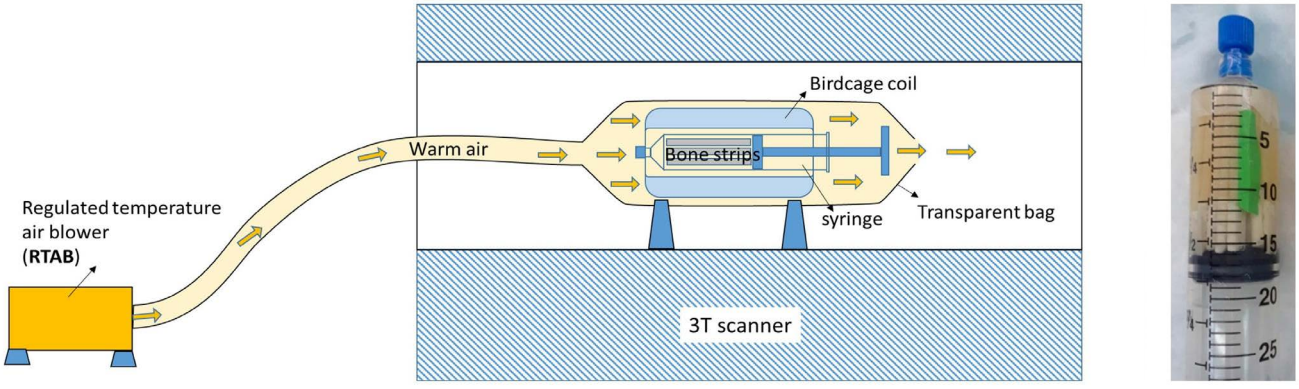

a b

Fig. 1. (a) Schematics of the MRI scanning setup which used the regulated temperature air blower (RTAB) to direct warm air at body temperature towards cortical bone specimens in a 30-ml syringe which was placed in a birdcage coil on a 3T clinical scanner. The warm air at 40˚ was directed through a flexible hose towards the transparent bag covering the coil and specimens. (b) Specimens were placed in a 30-ml syringe filled with Fomblin.

includes both bound and pore water protons. It is noted that if the macromolecular proton magnetization is partially saturated, the acquired water signal intensity decreases due to the magnetization transfer. Details of the two-pool MT modeling are described earlier (22, 23, 30). In this sense, all measurements and models were performed using the in-housed developed codes in MATLAB (version 2017, The Mathworks Inc., Natick, MA, USA).

Statistical Analysis

The differences in average single- and bi-component-T2*, single-component IR-T2* and T1 as well as MT modeling results were compared between the acquired room-temperature and body-temperature datasets using two-tailed paired t-student test. It is noted that the P-values below 0.05 were considered significant.

RESULTS

Figure 1a schematically shows the experimental setup for scanning bone specimens at body and room temperature. In comparison to the scans at body temperature, the desired temperature on the RTAB device was set to 40˚ to achieve the body temperature (37.5˚C) within the syringe. Additionally, the scanning process began one hour after turning on the RTAB device to ensure homogenous temperature distribution within the syringe. Subsequently, Figure 1b shows the fourteen bone specimens together with a rubber piece placed in the 30-ml syringe filled with Fomblin.

Figure 2 shows the UTE-MRI (TE = 0.032 ms) images of the fourteen studied cortical bone specimens at room and body temperatures. To begin with, there were three rubber pieces were placed in the syringe for calibration purposes. As has been shown, there were no clear differences were observed between images acquired at the different temperatures.

Figure 3a and b show the bi-component T2* decay fitting for a representative bone specimen (77-year-old male) at room and body temperatures, respectively. Figure 3c and d show single-component T1 recovery fitting for the same bone specimen at the two studied temperatures. Figures 3e and f present the two-pool MT modeling analyses for the same specimen at room and body temperatures, respectively. Generally speaking, the MT modeling was performed for five off-resonance frequencies (2, 5, 10, 20, and 50 kHz) and three MT saturation pulse power levels, including 400°, 600°, and 800°, which are indicated with blue, green, and red lines. The fitting curves followed the actual data points very well at both room and body temperatures. In this case, there were no clear differences in fitting accuracies that were found between datasets at room and body temperatures.

Table 1 presents average values of measured UTE-MRI biomarkers at room and body temperatures in addition

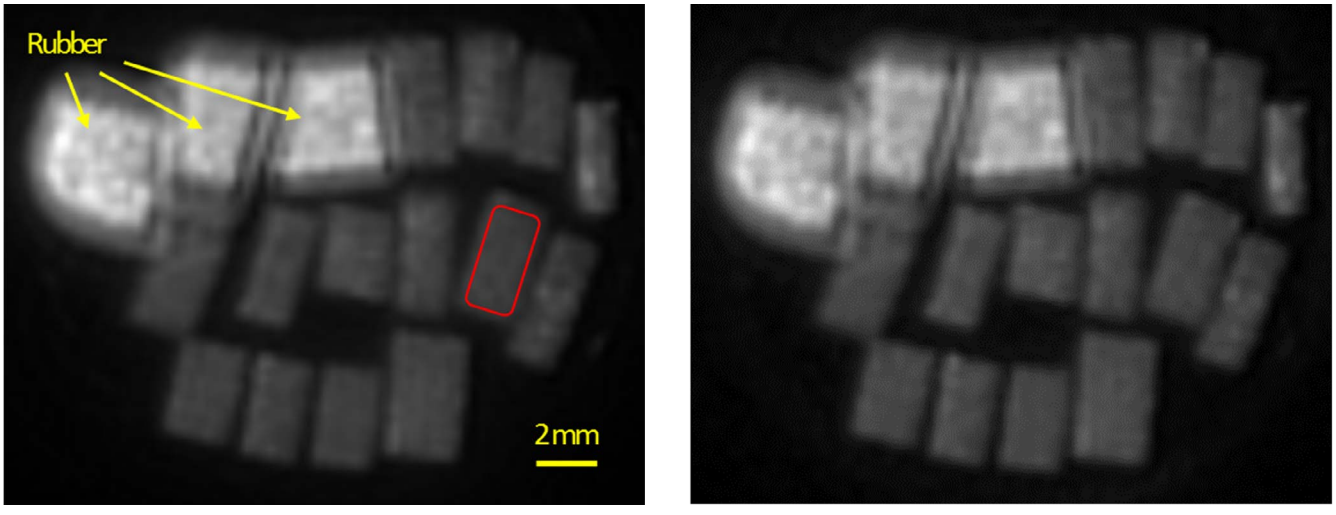

a b

Fig. 2. Ultrashort echo time MR images of fourteen cortical bone specimens in a 30-ml syringe (0.25 mm pixel size) at (a) room temperature and (b) body temperature. Bone specimens were placed in the syringe with three rubber pieces for further comparisons.

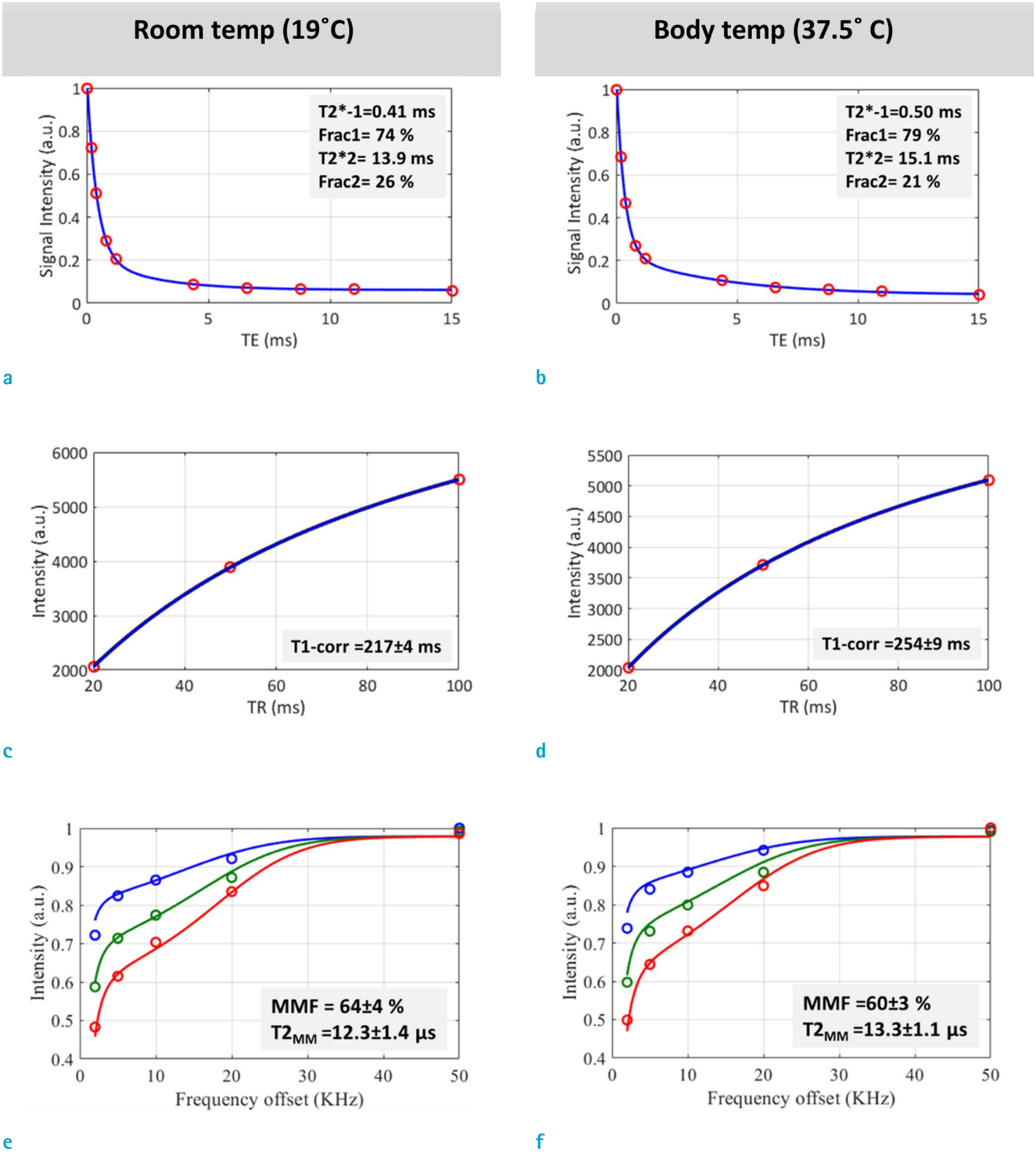

Fig. 3. T2* bi-component exponential fittings for a representative bone specimen (77-year-old, male, indicated in Fig. 1a) at (a) room temperature and (b) body temperature. T1 single-component exponential fitting for scans at (c) room temperature and (d) body temperature. The two-pool magnetization transfer modeling analyses at (e) room temperature and (f) body temperature using three pulse saturation power levels (400˚ in blue, 600˚ in green, and 800˚ in red) and five frequency offsets (2, 5, 10, 20, 50 kHz). Macromolecules fraction and macromolecular T2 refer to macromolecular fraction and macromolecular T2, respectively.

Table 1. Average T2*, T1, and MT Modeling Results at Room Temperature Compared with Body Temperature in Studied Fourteen Cortical Bone Specimens (63 ± 21 years old, 6 females)

			Bi-component					MT modeling	
	T2*-Single (ms)	IR-T2* (ms)	Frac1 (%)	$T2^*_S$ (ms)	Frac2 (%)	$T2^*_L$ (ms)	T1 (ms)	MMF (%)	$T2_{mm}$ (μs)
Room temp (19°C)	0.50 ± 0.06	0.30 ± 0.02	80 ± 5	0.38 ± 0.06	20 ± 5	10.9 ± 5.0	216 ± 17	63 ± 7	13 ± 1
Body temp (37.5°C)	0.54 ± 0.06	0.38 ± 0.04	86 ± 5	0.46 ± 0.05	14 ± 5	15.0 ± 8.6	242 ± 22	59 ± 9	14 ± 4
P (t-test)	< 0.01	< 0.01	< 0.01	< 0.01	< 0.01	0.01	< 0.01	0.04	0.26
Difference (%)	+7.5	+26.1	+6.3	+21.7	-25.8	+37.3	+11.9	-7.4	+10.8

Frac1 and T2*s = short component fraction and T2*; Frac2 and T2*L = long component fraction and T2*; IR-T2* = inversion recovery T2*; MMF = macromolecular fraction; $T2_{mm}$ = macromolecular T2

to their statistical differences obtained using two-tailed paired t-student test. All UTE-MRI measures but T2mm demonstrated significant differences between a review of the scans at room and body temperatures ($P < 0.05$). It is noted that the single-component T2*, IR-T2*, short component T2* (T2*S), long component T2* (T2*L), and T1 increased significantly as the temperature increased from room to body temperature. In the meantime, the MMF demonstrated significantly lower values at body temperature. Remarkably, it is shown that the short component fraction (Frac1) demonstrated significantly higher values at body temperature however the estimated T2* values for both components were increased.

DISCUSSION

This study examines the effect of temperature on the UTE-MRI biomarkers of *ex vivo* cortical bone samples. It is emphasized that the UTE-MRI techniques for *ex vivo* cortical bone assessment are routinely performed at room temperature as described in the literature. In this case, the UTE-MRI biomarkers have shown good correlations with bone microstructure and mechanics (7, 9, 10, 14-16, 21, 24). Extending the conclusion from *ex vivo* studies on the cortical bone specimens to future *in vivo* studies requires careful considerations of the resulting temperature differences. However, differences between *in vivo* and *ex vivo* studies are not limited to the differences noted with temperature in this case.

In this case, the homemade RTAB device provided stable and consistent air flow with the desired temperature during the scanning process. No clear difference was observed in the UTE-MRI image quality and the fitting accuracy between room and body temperature datasets. This result indicated consistent T/R coil performance at both studied temperatures and with the adequate RF shielding of the temperature controller.

The UTE-MRI biomarkers demonstrated significant differences between datasets at room and body temperature. T1, single-component T2*, IR-T2* and short and long component T2*s from bi-component analysis were significantly higher at body temperature, as compared with results at room temperature (Table 1). The IR-T2* and short-component T2* increases observed at body temperature indicated longer bound water relaxation times that resulted in less signal loss during data acquisition. Therefore, the short-component fraction from bi-component T2* analysis demonstrated higher values at body temperature. Moreover, the increase in T1 values due to the temperature increase might be higher for pore water, especially water residing in the larger pores, leading to higher short-component T2* fractions and lowering long-component T2* fractions (Table 1). The prevailing discipline notes that the MMF from the two-pool MT modeling revealed significantly lower values at body temperature, that was mainly due to higher T1 values used in the model.

In what follows, it is noted that increasing relaxation times by temperature increase was most likely due to the increased molecular and atomic motions, which agrees with the results in the literature where the tissue temperature difference was monitored using MRI relaxation times (25-29).

The temperature dependence of the MR relaxation times has been reviewed before as a useful MR thermometry technique in different biological tissues (28). In general, the T1 results from dipolar interactions of macromolecules and water molecules, which arise from their translational and

rotational motion (28). Such molecular motions enhance by temperature show an increase, which result in higher T1 at body temperature compared with room temperature. Additionally, the T1 temperature dependence is expected to be different for different tissues (28). A similar increase in T2 relaxation time with increasing temperature has been observed in aqueous solutions and bovine cortical bone (28). In this respect, a higher T1 has been also reported in bovine cortical bone specimens at higher temperature (26, 27, 29). On average, it is noted that the T1 showed 0.7-1.0 ms/˚C increase in bovine cortical bone in previous (26, 27, 29) T1 increase for the fourteen human studied specimens in this study was equal to 1.4 ± 0.3 ms/˚C which was significantly higher than reported values for bovine bone (26, 27, 29). The noted higher T1 increase in human bone specimen was most likely due to higher water and fat contents within the bone specimens.

Broadly speaking, the significant temperature-based differences in UTE-MRI measures suggest that the conclusions of *ex vivo* studies need to be modified before applying them to *in vivo* studies. Implementing a linear correction method on UTE-MRI measures based on the presented results in Table 1 might improve the validity of the techniques for future *in vivo* studies.

This study has some noted limitations. First, the body temperature in this study was set to 37.5˚ which may not be completely accurate for measurement of bone which exists at the body's extremities, such as at the location of the lower and upper limbs. Therefore, the expected temperature-based differences between *ex vivo* and *in vivo* studies depends on the studied cortical bone location in the body. For instance, the differences in the hip and spine may be higher than the differences in tibial and radius midshaft when measuring using this process. Second, this study only focused on temperature as one of the differences between the *in vivo* and *ex vivo* studies. However, other differences may have a reverse impact on the UTE-MRI biomarkers that can compensate for the measured temperature impact. For example, the fat percentage in the cortical bone proximity *in vivo* and potential chemical shifts can result in lower T2* values *in vivo*, as compared with the *ex vivo* bone specimens.

In conclusion, the temperature-based differences of the reviewed cortical bone UTE-MRI biomarkers as noted between the recorded body and room temperatures were investigated. Single-component T2*, IR-T2*, T2*S, and T2*L from bi-component analysis as well as T1 showed significantly higher values however MMF from MT modeling revealed significantly lower values at body temperature. The relaxation time increase per temperature unit for studied human cortical bone was higher than reported values for bovine bone as seen in the literature review. Higher relaxation times of the bound water at body temperature likely resulted in a lower signal loss during data acquisition, which led to higher values of Frac1 from the resulting bi-component analysis. This study highlights the need for careful considerations of the temperature differences before extending conclusion from *ex vivo* studies on cortical bone specimens to any future clinical applications. The presented results here can be used to implement a linear correction on UTE-MRI measures to improve the validity of the techniques for *in vivo* studies.

Conflict of Interest Statement

The authors have no conflicts of interest to declare.

Acknowledgments

The authors acknowledge grant support from NIH (1R21AR073496, R01AR0689871, R01AR062581-01A1) and VA Clinical Science and Rehabilitation R&D Awards (I01CX001388 and I01RX002604).

REFERENCES

1. Seifert AC, Wehrli FW. Solid-state quantitative (1)H and (31)P MRI of cortical bone in humans. Curr Osteoporos Rep 2016;14:77-86
2. Granke M, Does MD, Nyman JS. The role of water compartments in the material properties of cortical bone. Calcif Tissue Int 2015;97:292-307
3. Nyman JS, Ni Q, Nicolella DP, Wang X. Measurements of mobile and bound water by nuclear magnetic resonance correlate with mechanical properties of bone. Bone 2008;42:193-199
4. Chang EY, Du J, Chung CB. UTE imaging in the musculoskeletal system. J Magn Reson Imaging 2015;41:870-883
5. Du J, Bydder GM. Qualitative and quantitative ultrashort-TE MRI of cortical bone. NMR Biomed 2013;26:489-506
6. Lee H, Zhao X, Song HK, Zhang R, Bartlett SP, Wehrli FW. Rapid dual-RF, dual-echo, 3D ultrashort echo time craniofacial imaging: a feasibility study. Magn Reson Med 2019;81:3007-3016
7. Lu X, Jerban S, Wan L, et al. Three-dimensional ultrashort echo time imaging with tricomponent analysis for human cortical bone. Magn Reson Med 2019;82:348-355

8. Wan L, Zhao W, Ma Y, et al. Fast quantitative 3D ultrashort echo time MRI of cortical bone using extended cones sampling. Magn Reson Med 2019;82:225-236
9. Jerban S, Ma Y, Wan L, et al. Collagen proton fraction from ultrashort echo time magnetization transfer (UTE-MT) MRI modelling correlates significantly with cortical bone porosity measured with micro-computed tomography (muCT). NMR Biomed 2019;32:e4045
10. Rajapakse CS, Bashoor-Zadeh M, Li C, Sun W, Wright AC, Wehrli FW. Volumetric cortical bone porosity assessment with MR imaging: validation and clinical feasibility. Radiology 2015;276:526-535
11. Manhard MK, Nyman JS, Does MD. Advances in imaging approaches to fracture risk evaluation. Transl Res 2017;181:1-14
12. Diaz E, Chung CB, Bae WC, et al. Ultrashort echo time spectroscopic imaging (UTESI): an efficient method for quantifying bound and free water. NMR Biomed 2012;25:161-168
13. Wu Y, Dong Y, Jiang J, Li H, Zhu T, Chen S. Evaluation of the bone-ligament and tendon insertions based on Raman spectrum and its PCA and CLS analysis. Sci Rep 2017;7:38706
14. Bae WC, Chen PC, Chung CB, Masuda K, D'Lima D, Du J. Quantitative ultrashort echo time (UTE) MRI of human cortical bone: correlation with porosity and biomechanical properties. J Bone Miner Res 2012;27:848-857
15. Granke M, Makowski AJ, Uppuganti S, Does MD, Nyman JS. Identifying novel clinical surrogates to assess human bone fracture toughness. J Bone Miner Res 2015;30:1290-1300
16. Li C, Seifert AC, Rad HS, et al. Cortical bone water concentration: dependence of MR imaging measures on age and pore volume fraction. Radiology 2014;272:796-806
17. Johnson EM, Vyas U, Ghanouni P, Pauly KB, Pauly JM. Improved cortical bone specificity in UTE MR imaging. Magn Reson Med 2017;77:684-695
18. Chen J, Chang EY, Carl M, et al. Measurement of bound and pore water T1 relaxation times in cortical bone using three-dimensional ultrashort echo time cones sequences. Magn Reson Med 2017;77:2136-2145
19. Ma YJ, Lu X, Carl M, et al. Accurate T1 mapping of short T2 tissues using a three-dimensional ultrashort echo time cones actual flip angle imaging-variable repetition time (3D UTE-Cones AFI-VTR) method. Magn Reson Med 2018;80:598-608
20. Du J, Diaz E, Carl M, Bae W, Chung CB, Bydder GM. Ultrashort echo time imaging with bicomponent analysis. Magn Reson Med 2012;67:645-649
21. Chang EY, Bae WC, Shao H, et al. Ultrashort echo time magnetization transfer (UTE-MT) imaging of cortical bone. NMR Biomed 2015;28:873-880
22. Ma YJ, Tadros A, Du J, Chang EY. Quantitative two-dimensional ultrashort echo time magnetization transfer (2D UTE-MT) imaging of cortical bone. Magn Reson Med 2018;79:1941-1949
23. Ma YJ, Shao H, Du J, Chang EY. Ultrashort echo time magnetization transfer (UTE-MT) imaging and modeling: magic angle independent biomarkers of tissue properties. NMR Biomed 2016;29:1546-1552
24. Jerban S, Ma Y, Nazaran A, et al. Detecting stress injury (fatigue fracture) in fibular cortical bone using quantitative ultrashort echo time-magnetization transfer (UTE-MT): an ex vivo study. NMR Biomed 2018;31:e3994
25. Ozhinsky E, Han M, Bucknor M, Krug R, Rieke V. T2-based temperature monitoring in bone marrow for MR-guided focused ultrasound. J Ther Ultrasound 2016;4:26
26. Han M, Scott SJ, Ozhinsky E, et al. Assessing temperature changes in cortical bone using variable flip-angle ultrashort echo-time MRI. AIP Conference Proceedings 2017;1821, 060001
27. Ramsay E, Mougenot C, Kazem M, Laetsch TW, Chopra R. Temperature-dependent MR signals in cortical bone: potential for monitoring temperature changes during high-intensity focused ultrasound treatment in bone. Magn Reson Med 2015;74:1095-1102
28. Rieke V, Butts Pauly K. MR thermometry. J Magn Reson Imaging 2008;27:376-390
29. Han M, Rieke V, Scott SJ, et al. Quantifying temperature-dependent T1 changes in cortical bone using ultrashort echo-time MRI. Magn Reson Med 2015;74:1548-1555
30. Ma YJ, Chang EY, Carl M, Du J. Quantitative magnetization transfer ultrashort echo time imaging using a time-efficient 3D multispoke Cones sequence. Magn Reson Med 2018;79:692-700
31. Gurney PT, Hargreaves BA, Nishimura DG. Design and analysis of a practical 3D cones trajectory. Magn Reson Med 2006;55:575-582
32. Carl M, Bydder GM, Du J. UTE imaging with simultaneous water and fat signal suppression using a time-efficient multispoke inversion recovery pulse sequence. Magn Reson Med 2016;76:577-582
33. Ma YJ, Zhu Y, Lu X, Carl M, Chang EY, Du J. Short T2 imaging using a 3D double adiabatic inversion recovery prepared ultrashort echo time cones (3D DIR-UTE-Cones) sequence. Magn Reson Med 2018;79:2555-2563
34. Biswas R, Bae W, Diaz E, et al. Ultrashort echo time (UTE) imaging with bi-component analysis: bound and free water evaluation of bovine cortical bone subject to sequential drying. Bone 2012;50:749-755